Mitig Adapt Strateg Glob Change (2009) 14:85–99
DOI 10.1007/s11027-008-9152-7

ORIGINAL ARTICLE

Quantification of net primary production of Chinese forest ecosystems with spatial statistical approaches

Qianlai Zhuang · Tonglin Zhang · Jingfeng Xiao · Tianxiang Luo

Received: 5 April 2008 / Accepted: 23 July 2008 /
Published online: 12 August 2008

Abstract Net primary production (NPP) of terrestrial ecosystems provides food, fiber, construction materials, and energy to humans. Its demand is likely to increase substantially in this century due to rising population and biofuel uses. Assessing national forest NPP is of importance to best use forest resources in China. To date, most estimates of NPP are based on process-based ecosystem modeling, forestry inventory, and satellite observations. There are little efforts in using spatial statistical approaches while large datasets of in-situ observed NPP are available for Chinese forest ecosystems. Here we use the surveyed forest NPP and ecological data at 1,266 sites, the data of satellite forest coverage, and the information of climate and topography to estimate Chinese forest NPP and their associated uncertainties with two geospatial statistical approaches. We estimate that the Chinese forest and woodland ecosystems have total NPP of 1,325±102 and 1,258±186 Tg C year^{-1} in 1.57 million km^2 forests with a regression method and a kriging method, respectively. These estimates are higher than the satellite-based estimate of 1,034 Tg C year^{-1} and almost double the estimate of 778 Tg C year^{-1} using a process-based terrestrial ecosystem model. Cross-validation suggests that the estimates with the kriging method are more accurate. Our developed geospatial statistical models could be alternative tools to provide national-level NPP estimates to better use Chinese forest resources.

Q. Zhuang (✉) · J. Xiao
Department of Earth & Atmospheric Sciences, Purdue University, CIVIL 550 Stadium Mall Drive, West Lafayette, IN 47907-2051, USA
e-mail: qzhuang@purdue.edu

Q. Zhuang
Department of Agronomy, Purdue University, West Lafayette, IN 47907-2051, USA

T. Zhang
Department of Statistics, Purdue University, West Lafayette, IN 47906, USA

T. Luo
The Institute of Tibetan Plateau Research, Chinese Academy of Sciences, Beijing P.O. Box 2871, 100085, China

Keywords Net primary production · Chinese forest ecosystems · Spatial statistics · Ecosystem modeling · Satellite-derived NPP · MODIS

1 Introduction

Net primary production (NPP) is the net amount of carbon captured by land plants through photosynthesis during a certain time period. It determines the amount of energy available for transfer from plants to other levels in the trophic webs in ecosystems (Haberl et al. 2007). It is of fundamental importance to human kind because the largest portion of our food supply is from productivity of plant life on land, as is wood for construction and fuel (Melillo et al. 1993). Moreover, it has also been contemplated as biofuel sources in recent years around the world (e.g., Obersteiner et al. 2006). Its demand is likely to increase substantially in next few decades due to rising population and increase of biofuel consumption (Imhoff and Bounoua 2006). The increasing demand on NPP presents a great challenge to human society because of the limited arable land on earth and the adverse effects of changing climate on NPP.

China has the third largest land areas in the world, next only to Russia and Canada, but has a quarter of the world population. Specifically, China's human population has increased about 2.5 times over the past 50 years, yet the human population in forested areas has increased five fold (Zhang et al. 1999). The fast economic development and population rising unavoidably increase the demand of NPP of terrestrial ecosystems. For example, the East Asia harvests 685 million m^3 wood per year, where China is the dominant country with respect to human population and land areas (Haberl et al. 2007).

At the present, China has approximately 1.31 million km^2 forests and woodlands including bamboo (e.g., Pan et al. 2004). These forest ecosystems not only play an important role in the fast economic development, which supplies high timber demand, but also offset a large amount of fossil fuel carbon dioxide emissions in the country because of plant photosynthesis. Assessing Chinese forest NPP supply is an important step to best use Chinese forest resources and evaluate the role of forests in the global carbon cycle. To date, most existing studies focus on quantifying NPP at site-levels. For example, Ni et al. (2001) used site-level information to examine the individual site-based NPP and the correlation between climate factors and NPP and did not extrapolate their site-level results to national level. Although Luo (1996) made a preliminary attempt to extrapolate the site-level information to the Tibetan Plateau region, he has not yet estimated total NPP for the region or China as a whole. To our knowledge, the national estimates of NPP have mostly been provided using process-based terrestrial ecosystem modeling approaches to date (e.g., Xiao et al. 1998; Pan et al. 2001; Cao et al. 2003; Jiang et al. 1999; Ni 2003; Piao et al. 2005a). Geospatial statistical approaches appear as a powerful way to quantify Chinese forest NPP (e.g., Wang et al. 2005). In addition, combining satellite data and forest inventory data have also made a good progress in quantifying Chinese biomass and NPP in recent years (e.g., Fang et al. 1998, 2001, 2003; Feng et al. 2007; Piao et al. 2005b). There are little efforts in using spatial statistical approaches while large datasets of in-situ observed NPP are available for Chinese forest ecosystems.

Here, we make an attempt to use the surveyed NPP and satellite derived land-cover data with two geospatial statistical approaches, which have not been used to date, to estimate national forest NPP. Specifically, the two methods are a multiple linear regression method and a kriging method to derive spatially-explicit estimates of NPP at an 8 km×8 km resolution (Diggle et al. 1998; Cressie 1993). The data of surveyed NPP and associated ecological, geographical, and climatic factors were developed by Luo (1996). Next, we use a process-based Terrestrial Ecosystem Model (TEM; Zhuang et al. 2003) and the satellite-based forest distribution to estimate national NPP for Chinese forest ecosystems at a spatial resolution of 8 km×8 km. We then compare the NPP estimates of spatial patterns and their magnitudes of these approaches. To check our results, the MODIS-based NPP is compared with our estimates (Running et al. 2004). To better understand the NPP distribution in China, we further analyze the spatial patterns and magnitudes of NPP for different forest ecosystem types and sub-regions across China.

2 Method

To implement these statistical approaches, we first organize both site-level and spatially-explicit information on vegetation, soils, and climate for representative forest ecosystems across China (Luo 1996). To verify these estimates, we apply a process-based biogeochemistry model, the Terrestrial Ecosystem Model at an 8 km×8 km resolution for whole Chinese forest ecosystems to simulate NPP (TEM; Zhuang et al. 2003). We then compare our estimates with both process-based and geospatial statistical approaches to the satellite-based NPP (Running et al. 2004). Below we first detail how we implement these two spatial statistical approaches. Second, we describe how we conduct the TEM simulations. Finally, we describe how we compare these estimates.

First, to develop spatial statistical estimates, we organize the ecological data of forest and woodlands for 1,266 sites compiled from the continuous forest-inventory plots in China during 1970–1994 (Luo 1996). For each site, we obtain the information of its ecosystem type, location [longitude (Lo) and latitude (La)], elevation (*E*), annual average monthly air temperature (*T*) and precipitation (*P*), total plant NPP (TNPP), aboveground (ANPP), and belowground NPP (BNPP). These NPP data were obtained using biomass measurements and allometric regression equations for 98 tree species, 4,507 continuous forest-inventory plots with measurements of tree height and diameter breast height (DBH), and 1,616 stem samples from 180 tree species (Fig. 1). With these site-level data, we develop a linear regression model for each forest ecosystem type. The dependent variables include TNPP, ANPP, and BNPP. The independent variables include elevation, longitude, latitude, annual air temperature, annual precipitation, and vegetation type for the site. To extrapolate the site information to national level, we classify these NPP sites into six broad ecosystem categories comprised of (1) evergreen needleleaved forests; (2) evergreen broadleaf forests; (3) deciduous needleleaved forests; (4) deciduous broadleaf forests; (5) mixed forests; and (6) woody savannas. These broad classifications are based on the International Geosphere–Biosphere Programme (IGBP) classification system, which is widely used in empirical and modeling studies at regional, continental, or global scales. We therefore reclassified the forest types in Luo's forest inventory database to the six IGBP forest classes (Table 1). We thus totally obtain 18 linear regression models for three dependent variables and six ecosystem types with this method (see Table 2).

The regression method uses the following model to estimate NPP:

$$NPP_j = \mu_k + \beta_1 T + \beta_2 T^2 + \beta_3 P + \beta_4 E + \beta_5 L_O + \beta_6 L_a + \beta_7 E \times L_O + \varepsilon \tag{1}$$

where NPP_j represents the total TNPP, ANPP, or BNPP with j=1,2,3, respectively, μ_k indicates the intercept term for vegetation type k (k=1, …,6) and ε is an error term assumed identically and independently and normally distributed (Table 3). To obtain the coefficients

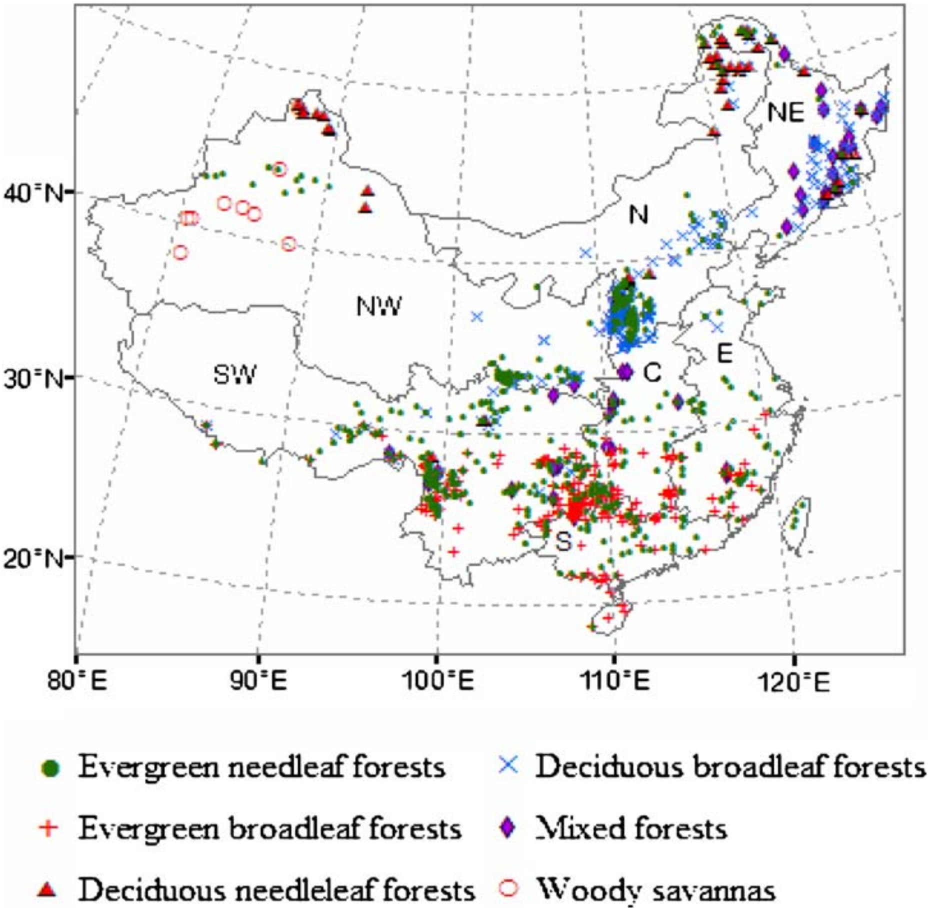

Fig. 1 The sample sites used in multiple regression and kriging methods across China. Sub-regions include Northern China (*N*); Northeastern China (*NE*); Northwestern China (*NW*); Central China (*C*); Eastern China (*E*); Southwestern China (*SW*); Southern China (*S*)

of Eq. 1 for each vegetation type, we conduct regression between the surveyed NPP and their independent variables of annual mean temperature, precipitation, elevation, longitude, and latitude. In addition, we also include the interactive term of elevation and longitude, which represents the elevational and longitudinal gradient from east to west in China. The *p*-values of the test for spatial dependence are all less than 0.0001 for TNPP, ANPP, and BNPP, respectively, which imply that dependent variables are all spatially dependent. The R^2 values of the regression models for TNPP, ANPP, and BNPP are 0.57, 0.36, and 0.57, respectively (Table 2).

Next, we extrapolate these linear regression models to Chinese forest ecosystems at a spatial resolution of 8 km×8 km using the spatially-explicit information on climate, vegetation type, elevation, and location. The spatially-explicit annual average temperature and precipitation for the 1990s are obtained from studies of Mitchell and Jones (2005). The data is similar to the climate data used in a mechanistic model application for Chinese forest NPP study (Ni 2003). The forest type map is derived from the International Geosphere–Biosphere Program (IGBP) Data and Information System (DIS) DISCover Database

Table 1 The IGBP land-cover classes and corresponding forest types in Luo's forest inventory database (Luo 1996)

IGBP classes	Forest types in Luo's database	Definition (Belward and Loveland 1996)
Evergreen needleleaved forests	Boreal/alpine Picea-Abies forest, Boreal *Pinus sylvestris* var. mongolica forest, temperate *Pinus tabulaeformis* forest, subtropical montane *Pinus yunnanensis* and *P. khasya* forest, subtropical *Pinus massoniana* forest, subtropical montane *Pinus armandii*, *P. taiwanensis* and *P. densada* forest, subtropical *Cunninghamia lanceolata* forest, subtropical montane Cupressus and Sabina forest	Tree canopy cover >60% and tree height >2 m. Most of the canopy is needle-leaved and remains green all year. Canopy is never without green foliage
Evergreen broadleaf forests	Sclerophyllous evergreen Quercus forest Tropical rainforest and monsoon forest	Tree canopy cover >60% and tree height >2 m. Most of the canopy is broad-leaved and remains green all year. Canopy is never without green foliage
Deciduous needleleaved forests	Boreal/temperate Larix forest	Tree canopy cover >60% and tree height >2 m. Most of the canopy is needle-leaved and deciduous
Deciduous broadleaf forests	Temperate typical deciduous broadleaved forest Temperate/subtropical montane Populus–Betula deciduous forest	Tree canopy cover >60% and tree height >2 m. Most of the canopy is broad-leaved and deciduous
Mixed forests	Subtropical mixed evergreen-deciduous broadleaved forest	Tree canopy cover >60% and tree height >2 m. Mixed evergreen and deciduous canopy
Woody savannas	Desert riverside woodland	Forest canopy cover between 30–60% and height >2 m

(Belward et al. 1999; Loveland et al. 2000). The 1 km elevation data are derived from the Shuttle Radar Topography Mission (SRTM) (Farr et al. 2007). The 1 km×1 km DISCover dataset is reclassified into our six broad ecosystem types and aggregated to 8 km×8 km resolution. The climate and elevation data are also re-sampled to 8 km×8 km spatial resolution.

The kriging method assumes that the error term ε (in Eq. 1) is spatially dependent with a stationary correlation function. Here we take the popular Matérn correlation function defined by $\rho_{a,b}(h) = \frac{a}{2^{v-1}\Gamma(v)}\left(\frac{h}{b}\right)^{v}\kappa_v\left(\frac{h}{b}\right)$ when $h>0$ and $\rho_{a,b}$ (0)=1, where h is the distance

Table 2 Coefficients of multiple linear regression models derived from NPP data and their environmental variables at field plots

	μ_i	β_1	β_2	β_3	β_4	β_5	β_6	β_7	β_8	R^2
NPP	μ_1	−1,387.1	18.2	0.59	0.31	0.49	7.35	14.19	−0.004	0.57
BNPP	μ_2	−3,13.4	3.0	0.13	0.025	0.06	1.51	3.14	−0.004	0.36
ANPP	μ_3	−1,073.7	15.2	0.46	0.28	0.43	5.84	11.04	−0.004	0.57

The dependent variables include TNPP, ANPP, and BNPP with units of gram C per square meter per year. The independent variables include air temperature, precipitation, elevation, longitude, latitudes and interactive terms of longitude and elevation.

Table 3 Coefficient μ_i for different forest ecosystems in the multiple linear regression method

	μ_1	μ_2	μ_3
Evergreen needleleaved forests	0.0	0.0	0.0
Evergreen broadleaved forests	223.4	38.9	184.5
Deciduous needleleaved forests	147.6	12.3	145.3
Deciduous broadleaved forests	163.4	21.6	141.9
Mixed forests	75.8	27.9	47.9
Woody savannas	48.8	18.1	30.7

between two points, Γ is the gamma function and κ_v is the modified Bessel function (Abramowitz and Stegun 1965). The parameter v is the smoothness parameter with a larger value corresponding to a smoother field. The parameter b is a scale parameter with a large value indicating a strong dependence and a small value indicating a weak dependence. The parameter a is between 0 and 1 with value less than 1 indicating the existence of nugget effect (Cressie 1993). Since the smoothness parameter v is hard to estimate and its changes do not affect the kriging prediction values, we chose v as the conventional value 1 in our study. Therefore, the correlation function has only two unknown parameters a and b (Tables 4 and 5).

Based on the correlation function, the kriging method predicts the response value for any unknown point in the study area using the minimum-mean-squared-prediction-error method that has been frequently used in spatial prediction of a Gaussian stationary random field (e.g., Cressie 1993). Here the kriging prediction of any pixel $(Y_\theta(S_u))$ in the study area is given by

$$Y_\theta(S_u) = X^t(S_u)\beta + r_\theta(S_u)^t R_\theta^{-1}(Y - X\beta) \tag{2}$$

with a variance estimation as

$$V_\theta(Y(S_u)|Y) = \sigma^2\left(1 - r_\theta(S_u)^t R_\theta^{-1} r_\theta(S_u)\right) \tag{3}$$

where $X(S)=(1, x_1(S), \ldots, x_{p-1}(S))$ is the vector of independent variables at locations of observations, β is the parameter vector of the independent variables, R_θ is the correlation matrix of observations, and $r_\theta(S_u)$ is calculated as

$$r_\theta(S_u) = (\rho_\theta(S_u - S_1), \ldots, \rho_\theta(S_u - S_n)). \tag{4}$$

Since we choose the Matérn correlation function, there are only two parameters contained in the correlation matrix R_θ as we can write $\theta=(a,b)$. Here, we estimate the parameter θ by the profile likelihood method (Murphy and van der Vaart 2000). When the

Table 4 Coefficients of regression equations for the kriging method derived from plot NPP data and their environmental variables

	μ_i	a	b	β_1	β_2	β_3	β_4	β_5	β_6	β_7	β_8	σ
NPP	μ_1	0.2785	219.74	−649.1	28.2	0.69	−0.16	−0.69	19.43	0.15	0.0025	19.5
BNPP	μ_2	0.429	55.63	−211.2	3.1	0.13	−0.015	0.94	2.6	0.01	−0.00002	0.68
ANPP	μ_3	0.2732	234.8	−520.7	26.3	0.56	−0.17	−1.44	18.0	0.14	0.002	15.6

The dependent variables include TNPP, ANPP, and BNPP with units of gram C per square meter per year. The independent variables include air temperature, precipitation, elevation, longitude, latitudes and interactive terms of longitude and elevation.

Table 5 Coefficient μ_i for different forest ecosystems in the kriging method

	μ_1	μ_2	μ_3
Evergreen needleleaved forests	0.0	0.0	0.0
Evergreen broadleaved forests	235	45.9	189.1
Deciduous needleleaved forests	130	11.2	118.6
Deciduous broadleaved forests	176.3	24.0	151.7
Mixed forests	75.4	33.3	43.3
Woody savannas	−277.9	−0.87	−274.1

estimate of θ is derived, we estimate the other parameter using the generalized least square method as

$$\beta = \left(X^t R_\theta^{-1} X\right)^{-1} X^t R_\theta^{-1} Y \tag{5}$$

and

$$\sigma^2 = \frac{1}{n-p} Y^t M_\theta Y \tag{6}$$

Where

$$M_\theta = R_\theta^{-1} - R_\theta^{-1} X \left(X^t R_\theta^{-1} X\right)^{-1} X^t R_\theta^{-1} \tag{7}$$

and $R_\theta = \left(\rho_\theta\left(\|S_i - S_j\|\right)\right)_{i,j=1,\ldots,n}$ is the correlation matrix of the observations, which is assumed invertible for all θ in the parameter domain. The correlation function $\rho_\theta(.)$, a spherical distance correlation (Stein 2005; Weber and Talkner 1993), is calculated by using the maximum likelihood estimation method (Murphy and van der Vaart 2000). Y is the vector of observations of dependent variables at locations S_1 to S_n. Where n is the total number of observation points, p is the dimension of independent variable which is 13 in our study. The $1-\alpha$ level confidence interval of the simple kriging prediction is also calculated (Cressie 1993).

Similar to using the multiple linear regression approach, to calculate the spatially-explicit forest ecosystem NPP in China, we use Eqs. 2 and 3 to calculate TNPP, ANPP, and BNPP and their confidence intervals with the independent variables for each pixel at an 8 km×8 km resolution. Specifically, in developing regression models of NPP using Eq. 1, we include all independent variables considered in our multiple linear regression method in addition to the spherical correlation defined as $\rho_\theta(.)$. Thus, we obtain other eighteen regression models with Eq. 1 for NPP, but with different values for ε. The intercepts and coefficients of these models are presented in Tables 3 and 4. These regression models are then extrapolated to whole Chinese forest ecosystems driven by spatially-explicit independent variable data used in the linear regression method.

To evaluate our statistical estimates, we simulate NPP with a process-based biogeochemistry model, the Terrestrial Ecosystem Model (TEM; Zhuang et al. 2001, 2002, 2003) using the spatially-explicit data of climate, vegetation, soil, and topography for whole Chinese forest ecosystems. In TEM, at each monthly time step, NPP is calculated as the difference between gross primary production (GPP) and plant autotrophic respiration (R_A). Algorithms of GPP and R_A are described elsewhere (McGuire et al. 1992; Zhuang et al. 2003). The version of TEM used here is different from the ones used in Pan et al. (2001) and Xiao et al. (1998) for quantifying Chinese terrestrial ecosystem carbon dynamics. The earlier version of TEM is an equilibrium model, which is driven with a long-term average climate; while the current TEM uses transient climate data and is incorporated with the effects of soil thermal dynamics on carbon and nitrogen dynamics.

To run TEM, we organize the data of atmosphere, vegetation, soil texture, and elevation at an 8 km×8 km resolution from 1901 to 2002. Specifically, the monthly air temperature, precipitation, and cloudiness are based on data developed by Climate Research Unit (CRU) at United Kingdom (Mitchell and Jones 2005). These data are re-sampled to 8 km×8 km spatial resolution from original 0.5°×0.5° resolution. We use the annual atmospheric CO_2 data for the period of 1901 to 2002 from our previous studies (Zhuang et al. 2003). The developed data of vegetation, soil texture, and elevation at resolution of 8 km×8 km are also used to drive TEM. The model parameters of the simulation are documented elsewhere (Zhuang et al. 2003). During the simulation, we first run TEM to equilibrium for an undisturbed ecosystem using the long-term averaged monthly climate and CO_2 concentrations from 1901 to 2002 for each grid cell. We then spin up the model for 120 years with the climate from 1901 to 1940 to account for the influence of climate inter-annual variability on the initial conditions of the undisturbed ecosystem. We then run the model with transient monthly climate data from 1901 to 2002. The simulated NPP during the 1990s is compared to our spatial statistical estimates.

To examine if our statistical and process-based estimates are reasonable, we also compare our results with the satellite-based NPP from the Net Primary Production Yearly L4 Global 1 km product derived from MODIS (MODerate Resolution Imaging Spectroradiometer) (Running et al. 2004). The satellite NPP is simply computed as gross primary production (GPP) minus maintenance respiration of leaves and fine roots and annual growth respiration. The satellite GPP is calculated as the fraction of photosynthetically active radiation absorbed by vegetation canopies, derived from a spectral vegetation index, multiplied by incident radiation and the conversion efficiency. We use the satellite NPP data from 2001 to 2003 to get annual average values for each pixel. We also aggregate the pixel-level NPP of forest ecosystems for each sub-region and major ecosystem types in China for comparison studies.

3 Results and discussion

Our multiple linear regression method estimates that the Chinese forest ecosystems have 1,325±102, 1,158±91, and 167±19 Tg C year^{-1} for TNPP, ANPP, and BNPP, respectively, in total 1.57 million km^2 forested areas (Table 5). The largest NPP regions include Southwestern China and Eastern China, accounting for more than 50% of the total NPP. On a per unit area basis, the simulated TNPP increases from 537 in Northern China to 1,121 g C m^{-2} year^{-1} in Southern China with national average of 843 g C m^{-2} year^{-1}. Aboveground NPP accounts for 87% of total NPP. For different forest ecosystems, the evergreen broadleaf forests have a total 79 Tg C year^{-1} in 0.17 million km^2 areas while mixed forests account for more than 55% of the total NPP. Woody savannas occupy the second largest forest areas and have total NPP of 333 Tg C year^{-1}. The TNPP, ANPP, and BNPP of kriging estimates are slightly lower, but their standard deviations are higher than the regression method (Table 6). Overall, the kriging method estimates the Chinese forests have 1,258±186 Tg C year^{-1}.

The estimates of TNPP with two geospatial statistical approaches are comparable to satellite-based estimates (1,035 Tg year^{-1}) for the 1990s (Table 6). But the national forest TNPP is higher than TEM simulation of 778 Tg C year^{-1} in 1.2 million km^2 forested areas. Using an ecosystem model, Cao et al. (2003) estimated that the Chinese terrestrial ecosystems NPP is between 2,860 and 3,370 Tg C year^{-1} during the period of 1981–2000. In their study,

Table 6 Regional estimates of TNPP, ANPP, and BNPP (Tg C per year) with two geospatial statistical methods, process-based modeling, and satellite-based approaches for different regions and different forest types in China

	Area	Regression			Kriging			TEM	MODIS
		TNPP	ANPP	BNPP	TNPP	ANPP	BNPP	TNPP	TNPP
Region									
Northern China	0.10	53.7	44.6	9.1	54.0	43.3	10.7	69.9	42.9
Northeastern China	0.21	117.0	99.0	18.0	115.3	97.8	18.4	178.8	105.9
Northwestern China	0.07	46.1	39.6	6.5	54.2	46.1	8.2	45.1	39.6
Middle China	0.20	179.2	157.5	21.7	163.9	141.6	22.5	104.8	115.3
Eastern China	0.27	286.8	251.7	35.1	287.3	250.8	36.1	133.8	185.3
Southwestern China	0.53	439.4	386.7	52.7	414.1	358.6	55.4	175.6	436.6
Southern China	0.18	201.7	177.7	23.9	163.4	141.8	22.2	69.7	108.9
Forest type									
Evergreen needleleaved forests	0.06	29.6	24.5	5.2	27.5	22.6	5.2	104.0	41.2
Evergreen broadleaved forests	0.17	78.5	65.8	12.7	72.9	59.7	13.5	29.5	157.8
Deciduous needleleaved forests	0.01	4.9	4.2	0.7	5.3	4.6	0.8	3.4	3.6
Deciduous broadleaved forests	0.04	23.9	20.5	3.4	27.9	24.0	4.0	176.4	22.7
Mixed forests	1.01	854.8	749.2	105.6	836.6	726.4	110.9	350.0	631.5
Woody savannas	0.27	333.0	293.4	39.6	287.4	247.2	40.1	114.9	177.5
Total	1.57	1,324.7±102.1	1,157.7±91.4	167.2±18.8	1,257.6±186.3	1,084.4±171.4	174.5±22.7	778.4	1,034.6

Forest areas are in units of million square kilometer.

they did not specifically provide the total estimates for forest ecosystems, but estimating NPP of 1,200 g C m^{-2} year^{-1} for the evergreen broadleaf forest, which is much higher than our estimates ranging from 429 to 462 g C m^{-2} year^{-1} with our geostatistical methods (Table 6). This may suggest that their total NPP estimates for forest ecosystems tend to be high. Xiao et al. (1998) estimated that the NPP for evergreen broadleaf forest is 890 g C m^{-2} year^{-1}, which is between our estimates and ones by Cao et al. (2003). In another model study, Pan et al. (2001) estimated that temperate deciduous forests, temperate broadleaved evergreen forests and tropical evergreen forests combined have a potential NPP of 2,530 Tg C year^{-1}, which puts their values to the upper end of all existing estimates.

Our spatially-explicit estimates of national forest NPP present a similar spatial pattern with other approaches (Fig. 2). Specifically, there is a north–south gradient of NPP since the temperature and precipitation tend to increase from north to south and there are more productive forests towards the south. All estimates for northern China have a similar pattern among different approaches. In contrast, the difference occurs in southern China. For instance, both MODIS and TEM estimates are lower in southern China in comparison to our geostatistical estimates. In addition, the estimates of standard deviations with both statistical methods show a large spatial variability (Fig. 3; regression one not shown). On a per unit area

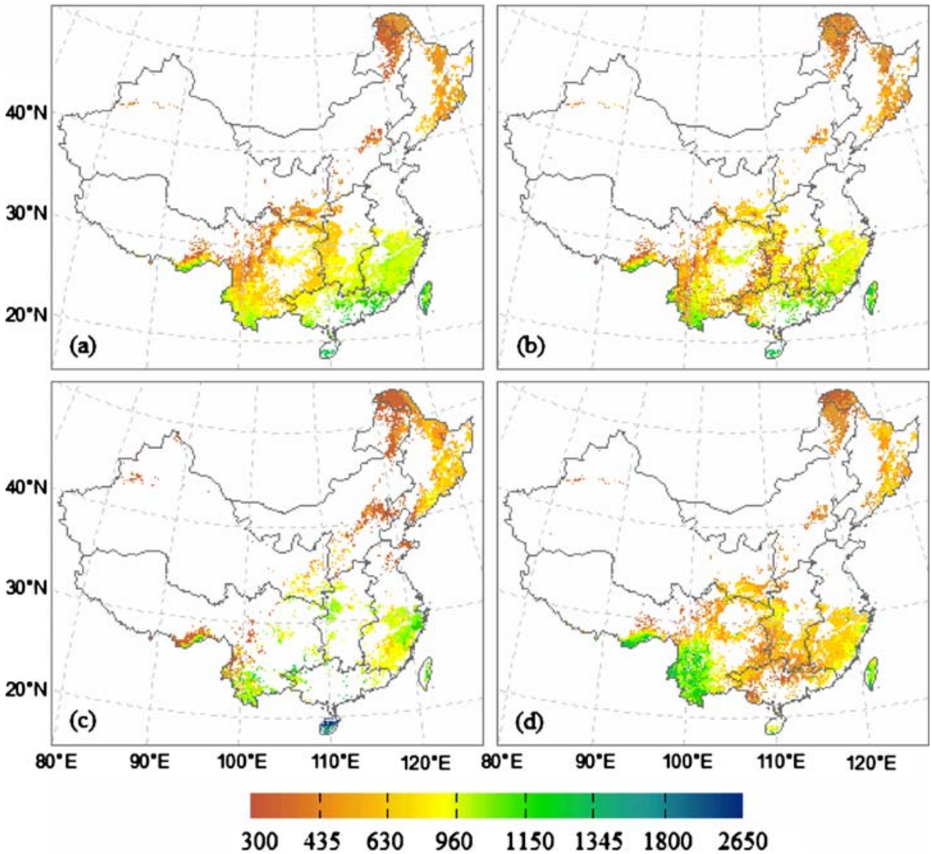

Fig. 2 Estimated spatial distribution of TNPP (gram C per square meter per year): **a** regression-based TNPP, **b** kriging-based TNPP, **c** TEM-based TNPP, and **d** MODIS-based TNPP

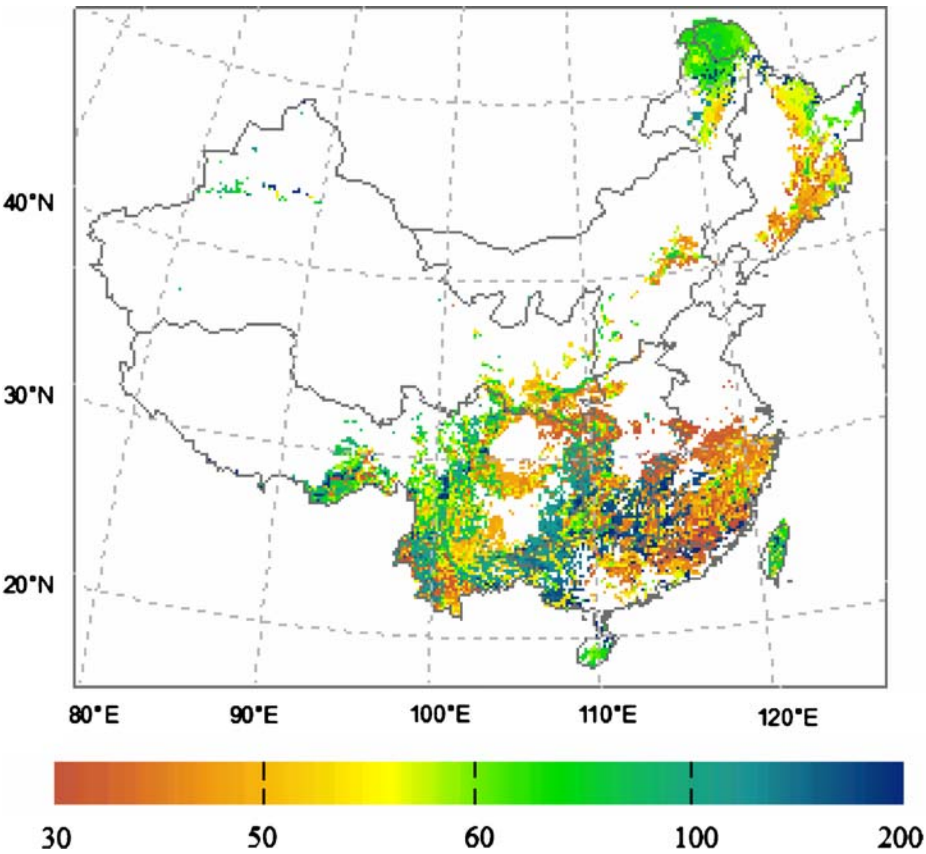

Fig. 3 Standard deviations of TNPP (gram C per square meter per year) in Chinese forest ecosystems estimated with the kriging method

basis, standard deviations of kriging estimates range from 10 to 142 g C m^{-2} $year^{-1}$. In general, the southern forests tend to have larger spatial variations of NPP than northern forest ecosystems. This may be due to the larger magnitudes of NPP in the south, the larger NPP results in the larger variations. In addition, the more diverse vegetation types in the south may also contribute to its larger spatial NPP variations.

In developing regression models for two spatial statistical methods, the step-wise regression procedure has been taken to select the final independent variables. Specifically, in the beginning, we use independent variables of normalized difference vegetation index (NDVI), leaf area index (LAI), and stand age in addition to those used in the current models. However we find there are no significant improvements to our regressions and spatial estimates by including NDVI, LAI, and stand age. The differences of annual national forest TNPP are less than 1% between with and without considering NDVI, LAI, and stand age. Thus, we do not include these two variables in our final calculations. However, both our process-based model and two geospatial statistical approaches may still overestimate the total NPP since we did not consider the stand age structure of forest ecosystems due to the lack of spatially-explicit data at a national level. The same reality of lacking of stand age data also occurred in an analysis of Chinese forest net ecosystem productivity by Wang et al. (2007). In these estimates, we assume that the Chinese forests are matured. Abundant studies have long recognized that the forest stand age is a controlling factor to NPP (e.g., McMurtrie et al. 1995; Gower et al. 1996). Thus, to improve our future estimates, the data of stand age structure for Chinese forest ecosystems affected by forest plantation, deforestation, fire and insect disturbances, and land-use changes are needed (e.g., Wang et al. 2001; Zhao and Zhou 2005).

To test the robustness of our geospatial statistical methods, we conduct the delete-one cross-validations (CV) according to

$$\mathrm{CV} = \sum_{i=1}^{n} \left(Y_i - \widehat{Y}_{(i)}\right)^2 \Big/ n \tag{8}$$

where $\widehat{Y}_{(i)}$ is the predicted value for the ith site by excluding Y_i in the model fitting. To compare the performance of multiple liner regression and kriging methods, we further compared the CVs for both methods. The CVs for the kriging method are 13.8%, 8.3%, and 13.6% lower than the regression method for TNPP, ANPP, and BNPP, respectively. This suggests that the kriging method provides more accurate predictions than the regression method.

To examine if our geospatial methods could be used for a prediction purpose, we apply our statistical models to the period from 1990 to 2002 driven by the spatially-explicit climate data (Mitchell and Jones 2005) for national forest ecosystems at an 8 km×8 km resolution. We find that the regression method provides a consistent higher estimate than the kriging method during the period (Fig. 4). The standard deviations are consistently bigger in the kriging method.

To examine the sensitivity of our geospatial statistical models, we conduct a set of simulations by alternating climate driving variables of air temperature and precipitation. Specifically, we disturb the climate: (a) change air temperature by 2°C, 0°C, and −2°C on

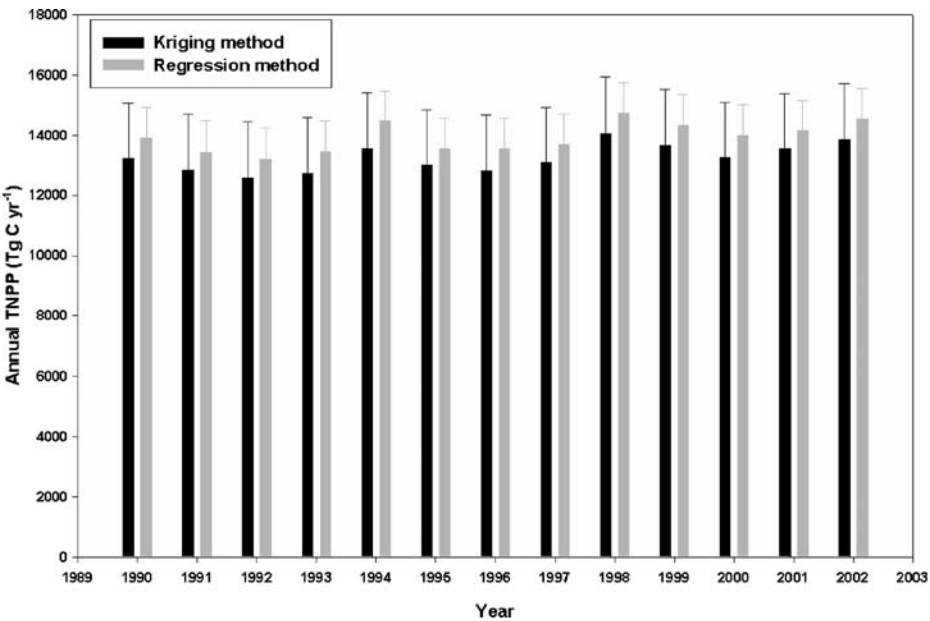

Fig. 4 Annual TNPP in Chinese forests estimated with a regression method and a kriging method. Standard deviations are derived from total 30,920 8 km-resolution pixels

original values; (b) change precipitation by 15%, 0%, and −15% on original values, (c) change both air temperature and precipitation according to (a) and (b) simultaneously. The ways to these changes for all forest grid cells are (a) with uniform changes for all cells and (b) randomly changes of air temperature with a normal random variable distribution with a mean 2°C, 0°C, and −2°C, respectively and a standard deviation 2; Precipitation is changed with a Gamma random variable distribution with (α, β)=(289/9, 340/9) for the 15% decrease and (α, β)=(529/9,460/9) for the15% increase. We find that, for both regression and kriging approaches, the total NPP of Chinese forests are estimated with a change ranging from a decrease 16% to an increase 17% in comparison to the standard simulations. This means that the uncertain climate driving data we used could lead to an error for total forest NPP ranging from 212 to 225 Tg C year^{-1} for the regression method and ranging from 201 to 214 Tg C year^{-1} for the kriging method.

The kriging approach used here is similar to other geospatial approaches, which have also considered the spatial dependence. Specifically, the kriging method used in our analysis has considered the spatial correlation function $\rho_\theta(.)$, a spherical distance correlation (Stein 2005; Weber and Talkner 1993). Other approaches include a geographically weighted regression (GWR) method (Fotheringham et al. 2002; Mennis 2006), which has been used to estimate Chinese NPP (e.g. Wang et al. 2005). In addition, the spatial autocorrelation approach is well known and has been shown effective in capturing spatial dependence (Ord 1975). The approach was originally used to analyze the spatial patterns for public health data (Elliott et al. 2000) and become a powerful tool for analyzing the spatial-dependence problems in environmental sciences (e.g., Zhang and Lin 2008; Lennon 2000; Lichstein et al. 2002).

4 Conclusion

In the study, we use the surveyed NPP data at a series of representative sites and associated ecological and environmental variables with a multiple linear regression method and a kriging method to quantify Chinese forest NPP at a national level. The regression method and kriging method estimate the Chinese forest NPP is 1,325±102 and 1,258±186 Tg C year^{-1}, respectively. Our developed geospatial statistical models could be good alternative tools to estimate the Chinese forest NPP to meet the needs to better use Chinese forest resources. In addition, we recommend that development of spatially-explicit data of stand age structure should be a priority to accurately quantify the Chinese forest NPP in the future.

Acknowledgments We thank two anonymous reviewers for valuable comments and suggestions. The study is funded by K. C. Wong research foundation, Hong Kong. The research is also supported in part by the National Science Foundation and the Department of Energy. The computing support is from the Rosen Center for Advanced Computing at Purdue.

References

Abramowitz M, Stegun I (1965) Handbook of mathematical functions, 9th edn. Dover, New York

Belward AS, Loveland T (1996) The DIS 1 km land cover data set. IGBP Glob Change News Letter 27:7–9

Belward AS, Estes JE, Kline KD (1999) The IGBP-DIS global 1-km land-cover data set DISCover: a project overview. Photogramm Eng Remote Sensing 65:1013–1020

Cao M, Prince SD, Li K, Tao B, Small J, Shao X (2003) Responses of terrestrial carbon uptake to climate inter-annual variability in China. Glob Change Biol 9:536–546. doi:10.1046/j.1365-2486.2003.00617.x
Cressie N (1993) Statistics for spatial data. Wiley, New York, p 900
Diggle PJ, Tawn JA, Moyeed RA (1998) Model-based geostatistics (with discussion). Appl Stat 47:299–350. doi:10.1111/1467-9876.00113
Elliott P, Wakefield J, Best N, Briggs D (2000) Spatial epidemiology. Oxford University Press, London
Fang JY, Wang GG, Liu GH, Xu SL (1998) Forest biomass of China: an estimate based on the biomass–volume relationship. Ecol Appl 8:1084–1091
Fang JY, Chen AP, Peng CH, Zhao SQ, Ci LJ (2001) Changes in forest biomass carbon storage in China between 1949 and 1998. Science 292:2320–2322. doi:10.1126/science.1058629
Fang JY, Piao S, Field CB, Pan Y, Guo QH, Zhou LM et al (2003) Increasing net primary production in China from 1982 to 1999. Front Ecol Environ 1(6):293–297
Farr TG et al (2007) The shuttle radar topography mission. Rev Geophys 45:RG2004. doi:10.1029/2005RG000183
Feng X, Liu G, Chen JM, Chen M, Liu J, Ju WM et al (2007) Net primary productivity of China's terrestrial ecosystems from a process model driven by remote sensing. J Environ Manage 85:563–573. doi:10.1016/j.jenvman.2006.09.021
Fotheringham AS, Brunsdon C, Charlton M (2002) Geographically weight regression. Wiley, New York
Gower ST, McMurtrie RE, Murty D (1996) Aboveground net primary productivity decline with stand age: potential causes. Trends Ecol Evol 11:378–382. doi:10.1016/0169-5347(96)10042-2
Haberl H, Heinz Erb K, Krausmann F, Gaube V, Bondeau A, Plutzar C et al (2007) Quantifying and mapping the human appropriation of net primary production in earth's terrestrial ecosystems. Proc Natl Acad Sci U S A 104:12942–12947. doi:10.1073/pnas.0704243104
Imhoff ML, Bounoua L (2006) Exploring global patterns of net primary production carbon supply and demand using satellite observations and statistical data. J Geophys Res 111:D22S12. doi:10.1029/2006JD007377
Jiang H, Apps MJ, Zhang YL, Peng CH, Woodard PM (1999) Modelling the spatial pattern of net primary productivity in Chinese forests. Ecol Modell 122(3):275–288. doi:10.1016/S0304-3800(99)00142-8
Lennon JJ (2000) Red-shift and red herrings in geographical ecology. Ecography 23:101–113. doi:10.1034/j.1600-0587.2000.230111.x
Lichstein JW, Simons TR, Shriner SA, Franzreb KE (2002) Spatial autocorrelation and autoregressive models in ecology. Ecol Monogr 72(3):445–463
Loveland TR et al (2000) Development of a global land cover characteristics database and IGBP DISCover from 1-km AVHRR data. Int J Remote Sens 21:1303–1330. doi:10.1080/014311600210191
Luo T (1996) Patterns of net primary productivity for Chinese major forest types and their mathematical models. Ph.D. Dissertation, Chinese Academy of Sciences, Beijing, China
McGuire AD, Melillo JM, Joyce LA, Kicklighter DW, Grace AL, Moore B III et al (1992) Interactions between carbon and nitrogen dynamics in estimating net primary productivity for potential vegetation in North America. Global Biogeochem Cycles 6:101–124. doi:10.1029/92GB00219
McMurtrie RE, Gower ST, Ryan MG, Landsberg JJ (1995) Forest productivity: explaining its decline with stand age. Bull Ecol Soc Am 76:152–154
Melillo JM, McGuire AD, Kicklighter DW, Moore B III, Vorosmarty CJ, Schloss AL (1993) Global climate change and terrestrial net primary production. Nature 363:234–240. doi:10.1038/363234a0
Mennis J (2006) Mapping the results of geographically weighted regression. Cartogr J 43:171–179. doi:10.1179/000870406X114658
Mitchell TD, Jones PD (2005) An improved method of constructing a database of monthly climate observations and associated high-resolution grids. Int J Climatol 25:693–712. doi:10.1002/joc.1181
Murphy SA, van der Vaart AW (2000) On profile likelihood. JASA 95:449–485 with discussion
Myneni RB, Dong J, Tucker CJ, Kaufmann RK, Kauppi PE, Liski J et al (2001) A large carbon sink in the woody biomass of Northern forests. Proc Natl Acad Sci U S A 98:14784–14789. doi:10.1073/pnas.261555198
Ni J (2003) Net primary productivity in forests of China: scaling-up of national inventory data and comparison with model predictions. For Ecol Manage 176:485–495. doi:10.1016/S0378-1127(02)00312-2
Ni J, Zhang X-S, Scurlock JMO (2001) Synthesis and analysis of biomass and net primary productivity in Chinese forests. Ann For Sci 58:351–384. doi:10.1051/forest:2001131
Obersteiner M, Alexandrov G, Benitez PC, McCallum I, Kraxner F, Riahi K et al (2006) Global supply of biomass for energy and carbon sequestration from afforestation/reforestation activities. Mitig Adapt Strategies Glob Change 11:1003–1021. doi:10.1007/s11027-006-9031-z
Ord K (1975) Estimation methods for models of spatial interaction. J Am Stat Assoc 70:120–126. doi:10.2307/2285387

Pan Y, Melillo JM, Kicklighter DW, Xiao X, McGuire AD (2001) Modeling structural and functional responses of terrestrial ecosystems in China to changes in climate and atmospheric CO_2. Acta Phytoecologica Sin 25(2):175–189

Pan Y, Lou T, Birdsey R, Hom J, Melillo J (2004) New estimates of carbon storage and sequestration in China forests: importance of age and method in inventory-based carbon estimates. Clim Change 67:211–236. doi:10.1007/s10584-004-2799-5

Piao SL, Fang JY, Zhou LM, Zhu B, Tan K, Tao S (2005a) Changes in vegetation net primary productivity from 1982 to 1999 in China. Global Biogeochem Cycles 19:GB2027. doi:10.1029/2004GB002274

Piao SL, Fang JY, Zhu B, Tan K (2005b) Forest biomass carbon stocks in China over the past 2 decades: estimation based on integrated inventory and satellite data. J Geophys Res 110:G01006. doi:10.1029/2005JG000014

Running SW, Nemani RR, Heinsch FA, Zhao M, Reeves M, Hashmoto H (2004) A continuous satellite-derived measure of global terrestrial primary production. Bioscience 54:547–560. doi:10.1641/0006-3568(2004)054[0547:ACSMOG]2.0.CO;2

Stein M (2005) Statistical methods for regular monitoring data. J. R Stat Soc B 67:667–687. doi:10.1111/j.1467-9868.2005.00520.x

Wang XK, Feng ZW, Ouyang ZY (2001) The impact of human disturbance on vegetative carbon storage in forest ecosystems in China. For Ecol Manage 148:117–123. doi:10.1016/S0378-1127(00)00482-5

Wang Q, Ni J, Tenhunen J (2005) Application of a geographically-weighted regression analysis to estimate net primary production of Chinese forest ecosystems. Glob Ecol Biogeogr 14(4):379–393. doi:10.1111/j.1466-822X.2005.00153.x

Wang S, Chen JM, Ju WM, Feng X, Chen M, Chen P et al (2007) Carbon sinks and sources in China's forests during 1901–2001. J Environ Manage 85:524–537. doi:10.1016/j.jenvman.2006.09.019

Weber RO, Talkner P (1993) Some remarks on spatial correlation function models. Mon Weather Rev 121:2611–2617. doi:10.1175/1520-0493(1993)121<2611:SROSCF>2.0.CO;2

Xiao X, Melillo JM, Kicklighter DW, Pan Y, McGuire AD, Helfrich J (1998) Net primary production of terrestrial ecosystems in China and its equilibrium responses to changes in climate and atmospheric CO_2 concentration. Acta Phytoecologica Sin 22(2):97–118

Zhang T, Lin G (2008) Cluster detection based on spatial associations and iterated residuals in generalized linear mixed models. Biometrics (in press)

Zhang P, Zhou X, Wang F (1999) Introduction to natural forest conservation program. China's Forestry Publishing House, Beijing, p 388 (in Chinese)

Zhao M, Zhou GS (2005) Estimation of biomass and net primary productivity of major planted forests in China based on forest inventory data. For Ecol Manage 207(3):295–313. doi:10.1016/j.foreco.2004.10.049

Zhuang Q, Romanovsky VE, McGuire AD (2001) Incorporation of a permafrost model into a large-scale ecosystem model: evaluation of temporal and spatial scaling issues in simulating soil thermal dynamics. J Geophys Res 106(D24):33,648–33,670. doi:10.1029/2001JD900151

Zhuang Q, McGuire AD, O'Neill KP, Harden JW, Romanovsky VE, Yarie J (2002) Modeling the soil thermal and carbon dynamics of a fire chronosequence in Interior Alaska. J Geophys Res 107(D1):8147. print 108(D1), 2003. doi:10.1029/2001JD001244

Zhuang Q, McGuire AD, Melillo JM, Clein JS, Dargaville RJ, Kicklighter DW, Myneni RB, Dong J, Romanovsky VE, Harden J, Hobbie JE (2003) Carbon cycling in extratropical terrestrial ecosystems of the Northern Hemisphere during the 20th Century: a modeling analysis of the influences of soil thermal dynamics. Tellus 55(B):751–776